Biogeochemistry
https://doi.org/10.1007/s10533-024-01136-0

Terrestrial and marine POC export fluxes estimated by ^{234}Th–^{238}U disequilibrium and δ^{13}C measurements in the East China Sea shelf

Qiangqiang Zhong · Dekun Huang · Qiugui Wang · Jinzhou Du · Fule Zhang · Jing Lin · Tao Yu

Received: 11 September 2023 / Accepted: 12 March 2024

Abstract The use of ^{234}Th–^{238}U disequilibrium has been widely employed to estimate the sinking flux of particulate organic carbon (POC) from the upper sea and ocean. Here, the deficits of ^{234}Th relative to ^{238}U in the water column and the carbon isotope signature (δ^{13}C) of POC in the East China Sea (ECS) Shelf were measured, which was used to distinguish the fraction of marine and terrestrial POC export fluxes. In the ECS Shelf, very strong deficits of ^{234}Th relative to ^{238}U were observed throughout the water column, with ^{234}Th/^{238}U activity ratios ranging from 0.158 ± 0.045 to 0.904 ± 0.068 (averaging 0.426 ± 0.159). The residence times of particle reactive radionuclide ^{234}Th (τ_{Th-T}) in the ECS shelf water varied between 9 and 44 days, which is significantly shorter than that in the continental slope area or the basin area. This phenomenon indicates that there is a more rapid particle scavenging process in the ECS shelf water compared to the continental slope and basin upper water. By applying a two-end-member mixing model based on the δ^{13}C, the fraction of terrestrial POC was estimated to be 0 to 74% (mean: 30 ± 22%) and the fraction of marine POC was in the range of 25% to 100% (mean: 70 ± 22%). Fluxes of marine and terrestrial POC settling to the seafloor exhibited significant spatial differences among different stations, ranging from 11 to 129 mmol C/m^2/day and from 2.6 to 38 mmol C/m^2/day, respectively. The averaged terrestrial POC fluxes in the southern and northern ECS Shelf were similar (~21 to 24 mmol C/m^2/day), while the marine POC fluxes in the north (86 ± 37 mmol C/m^2/day) were approximately four times higher than those in the south (26 ± 20 mmol C/m^2/day). Interestingly, the estimated export flux of both marine and terrestrial POC were approximately one order of magnitude higher than the previously reported burial fluxes of POC (ranging from 1.1 ± 0.1 to 11.4 ± 1.1 mmol C/m^2/day) in the underlying bottom sediments, indicating that the majority (>90%)

Responsible Editor: Christian Lønborg

Q. Zhong (✉) · D. Huang (✉) · F. Zhang · J. Lin · T. Yu (✉)
State Key Laboratory of Estuarine and Coastal Research, East China Normal University, Shanghai 200241, China
e-mail: zhongqiangqiang@tio.org.cn

D. Huang
e-mail: dkhuang@tio.org.cn

T. Yu
e-mail: yutao@tio.org.cn

Q. Zhong · J. Du
Third Institute of Oceanography, Ministry of Natural Resources, Xiamen 361005, China

Q. Zhong · D. Huang
Observation and Research Station of Island and Coastal Ecosystem in the Western Taiwan Strait, Ministry of Natural Resources, Xiamen 361005, China

Q. Wang
Key Laboratory for Water Quality and Conservation of the Pearl River Delta, Ministry of Education; School of Environmental Science and Engineering, Guangzhou University, Guangzhou 510006, China

Published online: 29 April 2024

of both terrestrial and marine POC exported from the upper water column are degraded in the sediments of the ECS Shelf. This "carbon missing" phenomenon can greatly be attributed to rapid decomposition by other processes (including microbial reworking, cross-shelf transport, and possible consumption by benthic organisms). Our findings highlight the dynamic nature of carbon cycling in the continental shelf and the need for further research to understand these processes and improve carbon budget assessments.

Keywords ^{234}Th–^{238}U disequilibrium · Carbon stable isotope · Continental shelf · POC export flux · ECS · Carbon neutrality

Introduction

In response to the global climate variation, China proposed a long-term goal of reaching its peak total CO_2 emissions around 2030 and achieving carbon neutrality before 2060 (Liu et al. 2022). Achieving carbon neutrality requires reducing carbon emissions and promoting carbon sequestration in terrestrial and marine ecosystems (Cheng 2020). The ocean, being an important carbon sink on Earth, stores approximately 44 times more carbon than the atmosphere (Friedlingstein et al. 2020). The "biological carbon pump" is a crucial mechanism that determines the size of the ocean's carbon sink. It involves the photosynthetic absorption of atmospheric CO_2 by ocean phytoplankton, which is then transported to the deep ocean as sinking biogenic particles, leading to long-term carbon sequestration in sediments (Buesseler et al. 2007). However, the most efficient carbon burial sites are found in the continental marginal seas. Despite accounting for only about 10% of the ocean's surface area, the continental shelves stores approximately 80% of the organic carbon (OC) burial within sediments (Muller-Karger et al. 2005) and contribute to around 30% of the total primary production of the global ocean (Eppley and Peterson 1979). Besides, the continental shelves receive huge amount of terrestrial OC in dissolved and particulate forms, as well as substantial nutrients exported from adjacent rivers. It has been estimated that large river-dominated marginal seas serve as hotspots to sequester terrestrial OC, with a burial flux of $(58 \pm 17) \times 10^{12}$ g C per year (Hedges and Keil 1995; Burdige 2005). Continental shelf regions, therefore, play a crucial role in the global carbon cycling and budget. Notably, they act as important marine carbon sinks, linking terrestrial and atmospheric carbon pools.

The East China Sea (ECS) holds significant importance as a marginal sea in the western Pacific Ocean. It stands out not only for its position as a major aquatic continuum connecting the largest continent (Europe-Asia) with the largest ocean (Pacific Ocean), but also due to the fact that approximately 10% of the global riverine sediment discharge enters this region and its adjacent sea areas, notably from the Changjiang and Huanghe rivers (Milliman and Meade 1983; Deng et al. 2006). The ECS Shelf receives large amounts of terrestrial materials (carbon, nutrient, etc.) from rivers, groundwater, and the atmosphere. The Changjiang River, which is the third-largest river on the earth, has an annual discharge of 0.9×10^{12} m^3 of water (Seo et al. 2022), 3.1×10^6 t of organic carbon (Wang et al. 2012), 500×10^6 t of sediments (Xu et al. 2018), 0.8×10^6 t of dissolved inorganic nitrogen (Shen and Liu 2009), and 20×10^6 t of dissolved inorganic carbon (Wu et al. 2003) onto the ECS shelf. The ECS Shelf exhibits a remarkably high level of primary production due to the substantial nutrient supply from the runoff of surrounding rivers and the Kuroshio upwelling (Wu et al. 2003; Gong et al. 2003; Seo et al. 2022).

Primary production in the ECS averages 33.3 mmol C/m^2/day, with significant seasonal variations (Gong et al. 2003). During summer, the maximum integrated primary production in the euphotic zone can reach as high as 173 mmol C/m^2/day in the Inner ECS Shelf near the Changjiang Estuary (Gong et al. 2003). These characteristics make the ECS Shelf an ideal area for studying the carbon cycle, including assessments of the carbon budget (Chen and Wang 1999; Deng et al. 2006), across-shelf carbon export (Oguri et al. 2003; Zhu et al. 2006), primary productivity (Ning et al. 1995; Gong et al. 2003), OC burial (Deng et al. 2006; Sun et al. 2020; Liu et al. 2023), and air-sea carbon exchange (Song et al. 2018). However, little is known about particulate organic carbon (POC) export fluxes (namely, export production) from upper sea in the ECS Shelf. In addition, considering that the ECS Shelf area is influenced not only by terrestrial POC input but also by high marine POC export (resulting from elevated primary production),

there is a lack of research on estimating POC export fluxes from the upper sea and differentiating between terrestrial and marine POC fluxes.

Due to its strong affinity for particles, ^{234}Th is usually depleted compared to ^{238}U in the upper water column (Black et al. 2019; Buesseler et al. 2020). This ^{234}Th–^{238}U disequilibrium has been extensively used to quantify the export flux of POC from the upper sea and ocean, utilizing measurements of ^{234}Th activity and POC concentration at the base of euphotic zone (Buesseler et al. 1992 2006; Hong et al. 2021; Yang et al. 2022). The stable carbon isotopic composition (δ^{13}C value) of organic matter has also been widely used to distinguish the relative proportions of marine and terrigenous OC in suspended particulate matter and surface sediments in estuaries, bays, and continental shelves (Hedges et al. 1988; Wu et al. 2003; Zhang et al. 2007; Seo et al. 2022). However, the combination of these two different types of geochemical tracers, ^{234}Th and δ^{13}C, to distinguish and quantitatively estimate the export fluxes of terrestrial and marine POC in coastal areas and continental shelves, particularly in the large river-dominated ECS Shelf, has received limited attention. This innovative combination provides a new assessment technology and has been successfully applied on the Mackenzie Shelf and in the Yellow Sea and Sea of Korea to estimate terrestrial and marine POC fluxes (Amiel and Cochran 2008; Seo et al. 2022). In this study, through field sampling, measurement, and reprocessing of published data in the Changjiang Estuary and adjacent areas, we aim to differentiate between terrestrial and marine source of carbon in the POC export flux from the ECS Shelf water and to figure out the fate and patterns of POC and OC budget with respect to carbon burial and decomposition in the ECS.

Methods

Study area, sampling, and data collection

The ECS is one of the largest marginal seas of the Pacific Ocean and is also a typical epicontinental sea covering a total area of approximately 0.77×10^6 km^2, of which 65% ($\sim0.55\times10^6$ km^2) has a water depth of less than 200 m (Deng et al. 2006). Our study stations were mainly located in the inner shelf of the ECS (see Fig. 1), which has an average water depth of 60 m

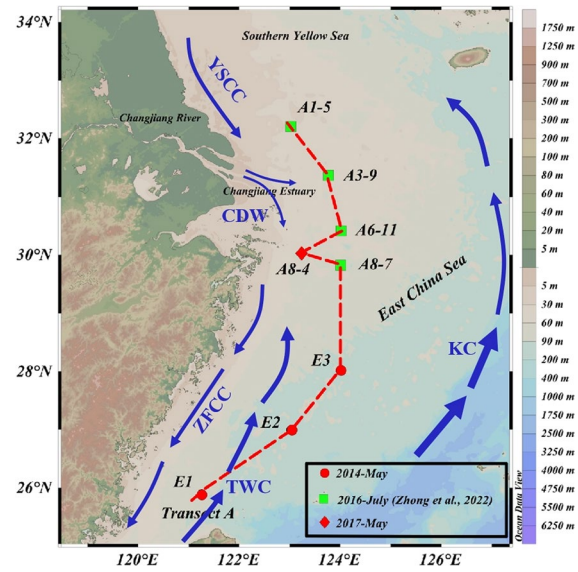

Fig. 1 Sampling stations in the inner shelf of the ECS (East China Sea) during the cruises in May 2014, July 2016 and May 2017. The stations visited during July 2016 were described in Zhong et al. (2022). And all these eight stations are connected to form the "Transect A" described in this paper

(Wang et al. 2008). The ECS shelf is characterized by a wide continental shelf with intricate hydrodynamics and high levels of primary production. It receives a large amount of nutrient-rich freshwater from the Changjiang River and also acquires significant nutrients from the upwelled subsurface water of the Kuroshio Current (KC). Consequenty, compared to other marginal seas worldwide, the primary productivity of the ECS shelf (primary production:108–997 mg C/m^2/day, average: 425 mg C/m^2/day, Gong et al. 2003) may be at a higher level. Additionally, the ECS shelf accumulates substantial amounts of sediments and associated terrigenous organic carbon transported from several large Chinese rivers, including the Changjiang River, Yellow River, Qiantang River, Ou River and Min River. This serves as another important carbon source in the ECS. It is estimated that the Changjiang River alone delivers $(2\sim5)\times10^6$ tons of terrigenous OC to the ECS (Yao et al. 2015). The complex current hydrodynamics of ECS is generally influenced by the Changjiang Diluted Water (CDW), the Yellow Sea Coastal Current (YSCC), the Zhejiang-Fujiang Coastal Current (ZFCC), and the Taiwan Warm Current (TWC) (see Fig. 1) (Su 2001; Zhou et al. 2015; Zhong et al. 2022).

Water samples for simultaneous determination of ^{234}Th and δ^{13}C were collected on three expeditions (May 2014, July 2016 and May 2017) in the area streching from the Changjiang Estuary to the adjacent ECS shelf (Fig. 1). In May 2014, three stations (E1, E2, and E3) in the southern ECS were sampled, and in May 2017, one station named A8-4 was sampled based on a shared cruise in the Changjiang Estuary. Data on ^{234}Th activities and δ^{13}C were obtained from Zhong et al. (2022) for four additional stations (A1-5, A3-9, A6-11, and A8-7) in the northern ECS, which was sampled in July 2016. However, Zhong et al. (2022) solely reported the activities and biogeochemical behaviors of ^{210}Po, ^{210}Pb, and ^{234}Th, without estimating the POC export fluxes at these four stations (for more details, please see the contents in Zhong et al. (2022)). For sampling, a total of 4–6 discrete water samples (depended on water depth) were collected from the surface to bottom using 30 L GoFlo bottles. The 30 L water samples were subdivided into 4 L for total ^{234}Th activities analysis, 8 L for particulate ^{234}Th activities analysis, and another 6 L for analysis of POC and δ^{13}C. To accurately determine the activities of total, dissolved (total-particulate), and particulate fractions of ^{234}Th, the 8 L subsamples for particulate ^{234}Th measurements were rapidly filtered through 25-mm diameter QMA filters (with 0.45 μm pore size) within 2 h of collection. Throughout the cruise, a Conductivity-Temperature-Depth (CTD) sensor (SBE 9/11, Sea-Bird Electronics, USA) was employed to record the salinity and temperature profiles in the water column.

Particulate ^{234}Th analyses

For the analysis of particulate ^{234}Th, the samples collected on the 25-mm diameter QMA filters were dried for 4 h at 60 °C. Subsequently, they were prepared and then mounted for beta counting (Amiel and Cochran 2008). The samples were counted onboard using a gas-flow proportional low background RISØ beta counter (Model GM-5–25, RISØ National Laboratory, Denmark). Multiple counts were performed over seven half-lives of ^{234}Th in the following six months to accurately determine the blank activities.

Total ^{234}Th analyses

To measure the total ^{234}Th, 4-L samples from Go Flo bottles were used, following the small-volume MnO_2 co-precipitation procedure of Buesseler et al. (2001) and Cai et al. (2006). The ^{230}Th as yield tracer was added to the samples, and both ^{234}Th and ^{230}Th were scavenged onto MnO_2 precipitate. The suspension of MnO_2 was collected onto a 25 mm diameter QMA filter and mounted for beta counting as done for the particulate samples. As the samples were unfiltered seawater, this method yields total ^{234}Th (including both particulate and dissolved forms). After the final background counting, thorium recoveries were obtained by adding 66 mBq ^{229}Th as recovery assessment tracer. After dissolving the precipitate and conducting an isolation and radiochemical purification of Th (Pike et al. 2005), the Th isotopes were electrodeposited onto a stainless-steel disc. Finally, this disc was counted in an ultra-low background alpha spectrometer (Alpha Analyst 7200, Canberra, USA). The recoveries for ^{230}Th in all the samples ranged from 64–95%, with an average of 74% (n = 39). The ^{238}U activity (dpm/L) is estimated from the U-salinity relationship of $[^{238}U](\pm 0.047) = 0.0786(\pm 0.00446) \times S\text{-}0.315(\pm 0.158)$ (Owens et al. 2011), and we use it to obtain ^{238}U activities from CTD salinity data for comparison with ^{234}Th (namely, ^{234}Th–^{238}U disequilibrium) in the East China Sea. Owens et al. (2011)'s equation was derived from the measured ^{238}U concentration and salinity (with a salinity range of 32–37) in the Atlantic and Southern Ocean. Although the coastal waters (like Changjiang Estuary) had a high particle abundance and low salinity characteristic, the bias of the calculated ^{238}U concentration by using Owens et al (2011)'s equation in the East China Sea would be controlled within the allowable error of 10% for low salinity (20–32).

POC and $\delta^{13}C_{POC}$ analyses

The 6-L seawater samples collected for determining POC and $\delta^{13}C_{POC}$ value were immediately filtered through pre-combusted (450 ℃) and pre-weighed QMA filters on the research ship. These filters were specifically treated to remove any calcium carbonate by exposure to concentrated hydrochloric acid (HCl) fumes overnight. After drying, the filters were tightly packed into tin cans. The C contents (expressed in

μmol C/L) and $\delta^{13}C_{POC}$ values were measured on a DELTA Plus XP isotopic ratio mass spectrometer (Thermo Electron Corporation, Germany). $\delta^{13}C_{POC}$ is reported as ‰-deviation from the carbon isotope composition of the international Vienna Pee Dee Belemnite standard. The precision of the analysis is ± 0.2‰ for $\delta^{13}C$ (Wu et al. 2003).

Results

^{234}Th activity, salinity, ^{238}U activity, POC concentration as well as $\delta^{13}C_{POC}$ and $^{234}Th/^{238}U$ activity ratio in the water column of the ECS inner shelf are presented in Appendix Table S1. In an attempt to obtain regional and depth-related variations in the water column, all data were plotted by using a linear kriging technique to grid the data in a software named Ocean Data View (Schlitzer 2020).

Salinity and ^{238}U

Latitudinal section patterns of salinity and ^{238}U activity concentration are shown in Fig. 2. Five stations in the northern region close to the Changjiang Estuary (A1-5, A3-9, A6-11, A8-4 and A8-7) have lower salinity, while the other three stations in the southern region have a stable salinity of ~ 34 (Fig. 2a) and the corresponding ^{238}U activity concentration is also stable at 2.40 ± 0.07 dpm/L (Fig. 2b). Salinity data at stations A1-5, A3-9, A6-11, A8-4 and A8-7 clearly show the influence of freshwater from the Changjiang River and Qiantang Jiang River on ^{238}U, with calculated ^{238}U values that are 1.45 ± 0.04–1.84 ± 0.06 dpm/L (Fig. 2b), at a salinity of 20–25 (Fig. 2a). From Fig. 2a, it can clearly be seen that more saline seawater invades the north along the seafloor from the south. Thus, ^{238}U stratification is especially evident at stations in the northern part, below 10 m, ^{238}U values approach 2.4 dpm/L as salinity increased to 32.5 (Fig. 2a).

Distributions of particulate and total ^{234}Th

Figure 3 displays the depth-related distributions of particulate (^{234}Th–P) and total ^{234}Th (^{234}Th–T) activities along the Transect A in the ECS inner shelf. ^{234}Th–P activities ranged from 0.07 ± 0.01 dpm/L to 0.64 ± 0.03 dpm/L (Fig. 3). At most stations, ^{234}Th–P were low in the upper 30 m and were high at depths near the sea bottom (Fig. 3), showing the possible influence of re-suspended bottom sediments on

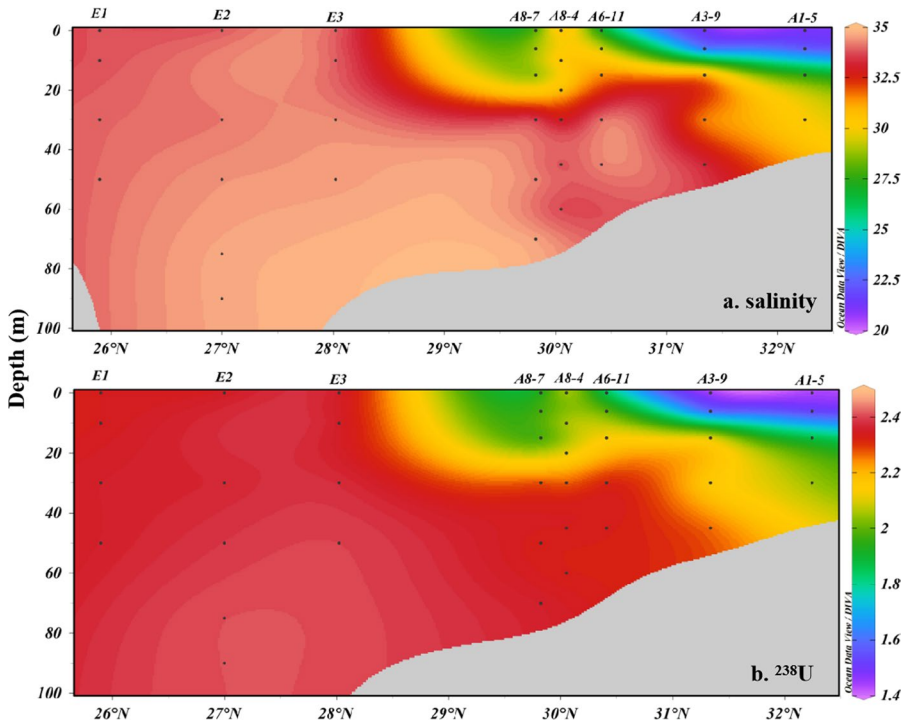

Fig. 2 Depth distributions of **a** salinity and **b** ^{238}U (dpm/L) in the Transect A (see Fig. 1) in the ECS (East China Sea) inner shelf

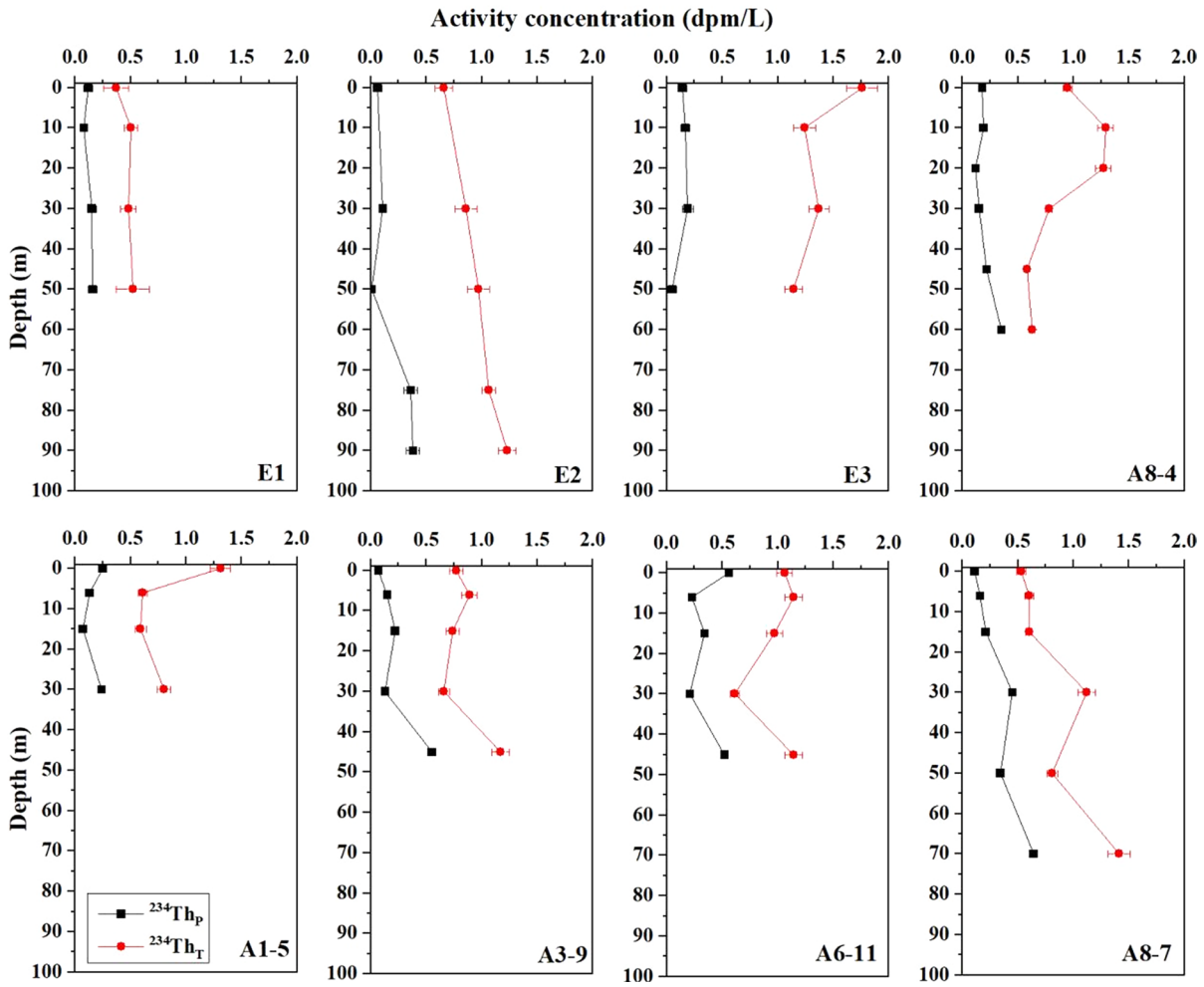

Fig. 3 Vertical distributions of ^{234}Th–P (particulate ^{234}Th) and ^{234}Th–T (total ^{234}Th). The location of different station name can be found in Fig. 1

^{234}Th–P activity. Total ^{234}Th activities varied from 0.37 ± 0.10 dpm/L to 1.75 ± 0.13 dpm/L (Fig. 3). Particulate ^{234}Th activity accounts for < 5%-56% (mean value: 26%) of the total ^{234}Th activity, indicating that dissolved ^{234}Th is the main form of thorium in the ECS shelf water. The southern region exhibits a clear increasing trend in total ^{234}Th activities with increasing depth, as depicted in Fig. 3. In contrast, the northern stations show low values of total ^{234}Th activities in the middle water column, with high values occurring in the upper and near-bottom waters. This suggests a significant particle export process in the surface and subsurface waters of the ECS inner shelf, as indicated by the low ^{234}Th feature in the upper and middle waters.

POC contents and carbon isotope distributions in filterable particles

POC concentrations ranged from a low value of 2.54 ± 0.08 μmol/L to a high value of 199 ± 6 μmol/L (Fig. 4a). Distribution pattern of POC concentration shows two general features. One is that POC concentrations decreased with increasing water depth at all stations, displaying the characteristics of higher POC levels in the surface waters and lower POC levels in the deeper layers. Another feature is that POC concentration were higher in the north part and lower in the south part of the study area. Specifically, POC concentrations at five stations (A8-7, A8-4, A6-11, A3-9 and A1-5) in the north region (8–199 μmol/L)

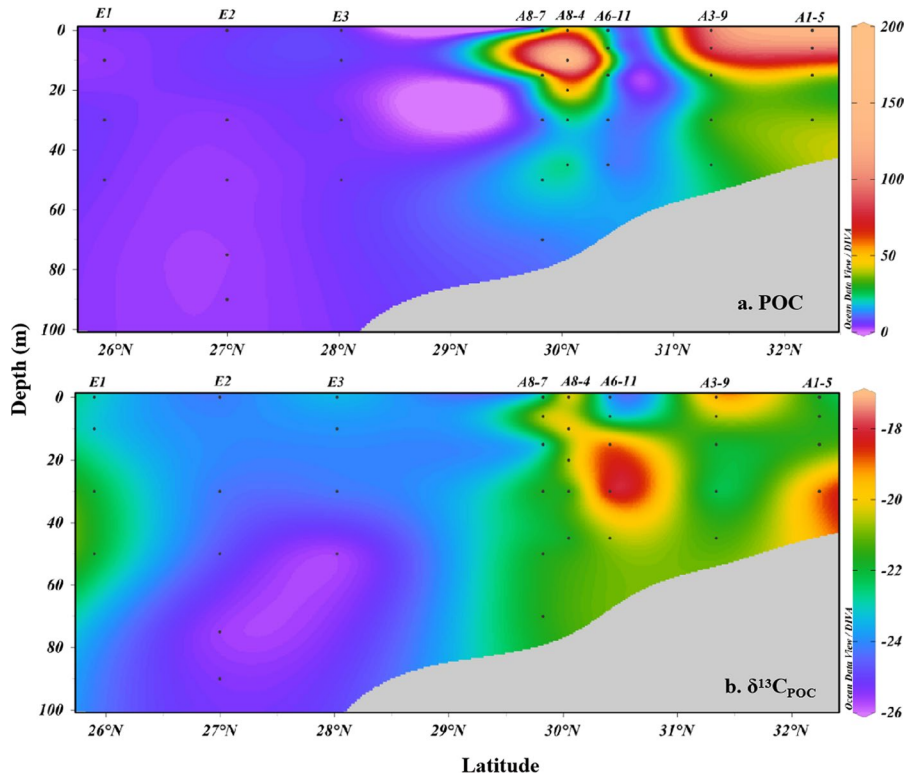

Fig. 4 Vertical distributions of **a** POC (particulate organic carbon) concentration (μmol/L) and **b** $\delta^{13}C_{POC}$ (ratio of carbon stable isotope) values (‰) for the Transect A in the ECS (East China Sea) inner shelf. And the location of different station name can be found in Fig. 1

were significantly higher than the POC concentrations at the three stations (E1, E2 and E3) in the southern region (2.53–6.66 μmol/L). The highest POC concentrations were observed at 10 m of station A8-4 and in the 0–10 m layers at station A1-5 and A3-9 (Fig. 4a). These elevated POC concentrations at specific depths are likely related to phytoplankton blooms occurring in the Changjiang Estuary. The input of nutrients from the Changjiang River and favorable environmental conditions can promote the growth of phytoplankton, leading to higher POC concentrations in the vicinity of the estuary.

The $\delta^{13}C_{POC}$ values exhibit clear regional variability. The overall range in $\delta^{13}C_{POC}$ for the > 0.45-μm particle size fraction was -17.6‰ to -25.7‰ with an average of -22.1 ± 2.0‰ (Fig. 4b). Horizontally, there is a distinct pattern in the $\delta^{13}C_{POC}$ values across the water columns. The $\delta^{13}C_{POC}$ are relatively heavier in the northern regions (-17.6 to -24.1‰), while they are lighter in the southern region (-21.8 to -25.7‰) (Fig. 4b). Vertically, different stations show varying patterns in the $\delta^{13}C_{POC}$ values within the > 0.45 μm fraction. At stations A1-5, A6-11, A8-7, and E1, the $\delta^{13}C_{POC}$ values become progressively heavier towards the near-bottom layer. In contrast, at stations A3-9, A8-4, E2, and E3, the $\delta^{13}C_{POC}$ values become lighter with increasing depth (Fig. 4b).

Discussion

Spatial distribution features of water column ^{234}Th–^{238}U disequilibrium

The activity ratios of ^{234}Th–T to ^{238}U (i.e., $^{234}Th/^{238}U$ AR) provide information about the ^{234}Th–^{238}U disequilibrium characteristics in the water column (see Fig. 5). The depth distribution of $^{234}Th/^{238}U$ AR is consistent with the section pattern of total ^{234}Th (see Fig. 3c and Fig. 5). The $^{234}Th/^{238}U$ AR values varied from 0.158 ± 0.045 to 0.904 ± 0.068 (averaging 0.426 ± 0.159, n = 39). These values indicate strong deficiencies of ^{234}Th relative to ^{238}U throughout the water column at all stations. A stratified structure of $^{234}Th/^{238}U$ disequilibrium was evident in the northern region. For example, at stations from A8-4 to A1-5, the surface $^{234}Th/^{238}U$ ARs were relatively high at the level of 0.5–0.8. However, in the middle water

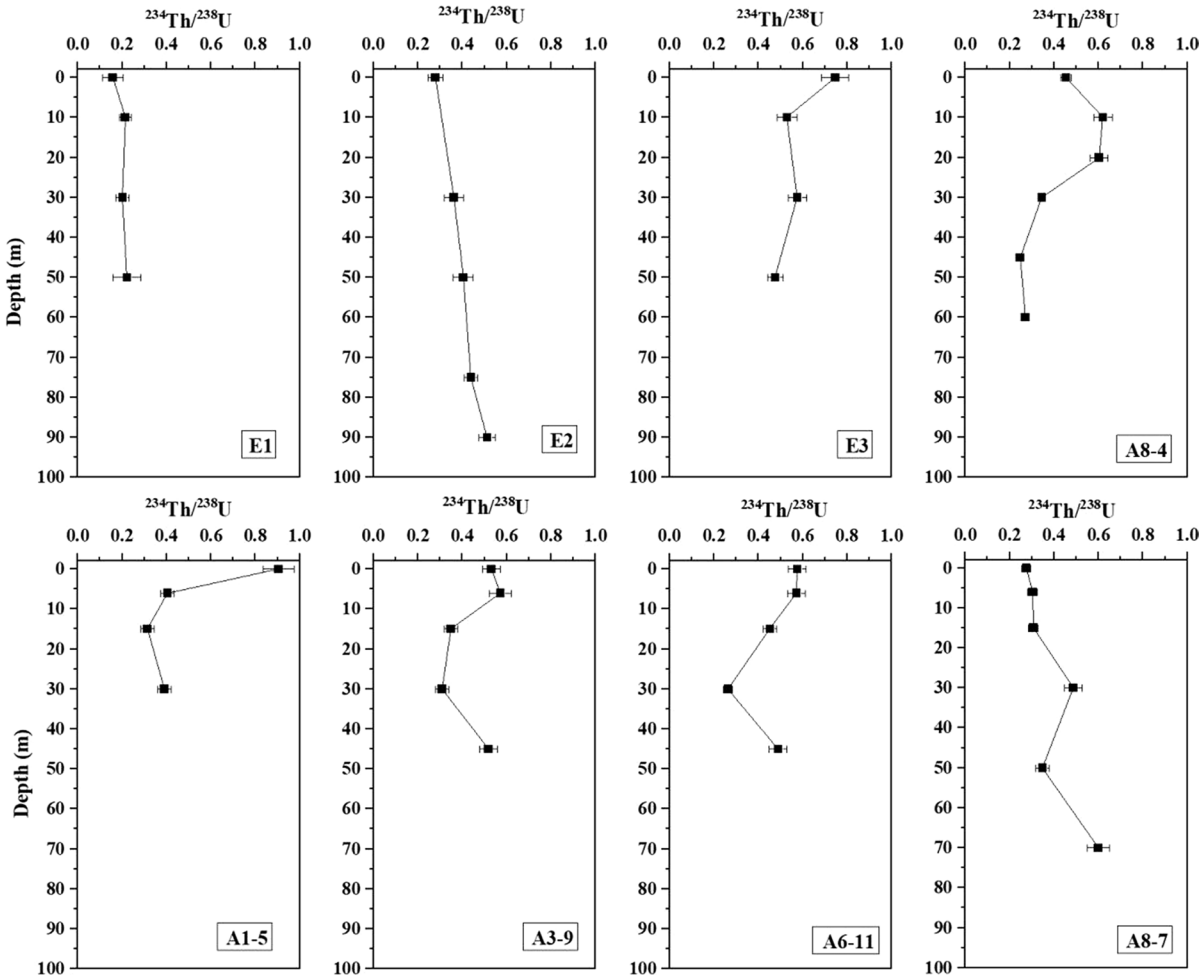

Fig. 5 Vertical distributions of total $^{234}Th/^{238}U$ AR (activity ratio) in the Transect A in the ECS (East China Sea) inner shelf. The location of different station name can be found in Fig. 1

(15–50 m), a remarkable decrease in ^{234}Th activities was observed (Fig. 3c), resulting in the $^{234}Th/^{238}U$ ARs as low as 0.2–0.3 (Fig. 5). At the near bottom depths, the $^{234}Th/^{238}U$ ARs increased again to ~ 0.5. Another notable feature of the total $^{234}Th/^{238}U$ AR distribution was observed in the upper 50 m at stations E1 and E2 in the south. These stations showed enhanced ^{234}Th deficiency relative to ^{238}U ($^{234}Th/^{238}U$ ratio of ~ 0.2). This phenomenon suggests the occurrence of the substantial ^{234}Th scavenging, possibly due to enhanced POC export production prior to sampling.

In natural oxic seawater, uranium (U) exists primarily as a highly soluble and stable carbonate complex, $UO_2(CO_3)_3^{4-}$, in the form of U(VI) (Djogić et al. 1986). Unlike soluble ^{238}U, thorium (Th) in its stable oxidation state (Th(IV)) is highly particle reactive in seawater and tends to adsorb onto lithogenic and marine particles, leading to its removal through article sinking (Santschi et al. 2006). This fundamental difference in the behavior of U and Th results in ubiquitous deficits of ^{234}Th relative to ^{238}U in particle-rich aquatic environments such as coastal and marginal seas, as well as the euphotic zone of the open ocean (Buesseler et al. 1992; Feng et al. 2021; Yang et al. 2022). From the five stations (A1-5, A3-9, A6-11, A8-4 and A8-7, Fig. 1) located in the north region of the study area near the Changjiang Estuary (shallow water depth: < 50 m), the $^{234}Th/^{238}U$ ARs were higher than 0.4 in the upper 20 m of the water

column. However, in the middle water layers, the $^{234}Th/^{238}U$ AR values dropped to as low as 0.2–0.3, showing enhanced scavenging and removal of ^{234}Th from the middle layers than in the surface (Fig. 5). In the near-bottom layers, the occurrence of a submarine nepheloid layer caused by sediment resuspension led to elevated ^{234}Th–P activity concentrations of approximately 0.5–0.6 dpm/L (Fig. 3a) and an increase in the $^{234}Th/^{238}U$ ARs to around 0.5 (Fig. 5). In contrast, the three stations (E1, E2, and E3) located in the south region were relatively deep up to approximately 100 m. Due to the efficient particle scavenging of ^{234}Th, the ^{234}Th–P activity concentrations in the water above 60 m at stations E1 and E2 were as low as 0.1–0.2 dpm/L, resulting in $^{234}Th/^{238}U$ ARs of approximately 0.2 in the water above 50 m (Fig. 5). However, at station E3, also located in the south, the activity concentration of ^{234}Th–D was much higher than at the other stations, indicating a strong process of ^{234}Th dissolution in the water column. This phenomenon was likely related to the intense decomposition of sinking particles from the upper seawater at station E3.

To provide a comprehensive understanding of the ^{234}Th–^{238}U disequilibrium characteristics from coastal seas to open seas, an analysis of averaged $^{234}Th/^{238}U$ ARs in the upper 100 m of the seawater column in the ECS and its adjacent seas was conducted (see Fig. 6). The results showed that, on average, the total $^{234}Th/^{238}U$ ARs increased and approached unity with increasing distance from the coastline (Fig. 6a), and the $^{234}Th/^{238}U$ AR values in the deep slope/basin area were much higher than those in shallow shelf or coastal seas (Fig. 6b). Specifically, in the SCS, the $^{234}Th/^{238}U$ ARs are in the following order: nearshore region (Daya Bay: 0.472 ± 0.128) < Mindoro Strait in Sulu Sea (0.498 ± 0.089) < shelf and slope area (northern SCS shelf, 0.780 ± 0.174) < central basin (southern SCS basin, 0.920 ± 0.124) (Wei and Hung 1998; Cai et al. 2008; Chen et al. 2008; Feng et al. 2021) (Fig. 6b). Similarly, in the Inner ECS Shelf, the $^{234}Th/^{238}U$ ARs in the upper 100 m water column

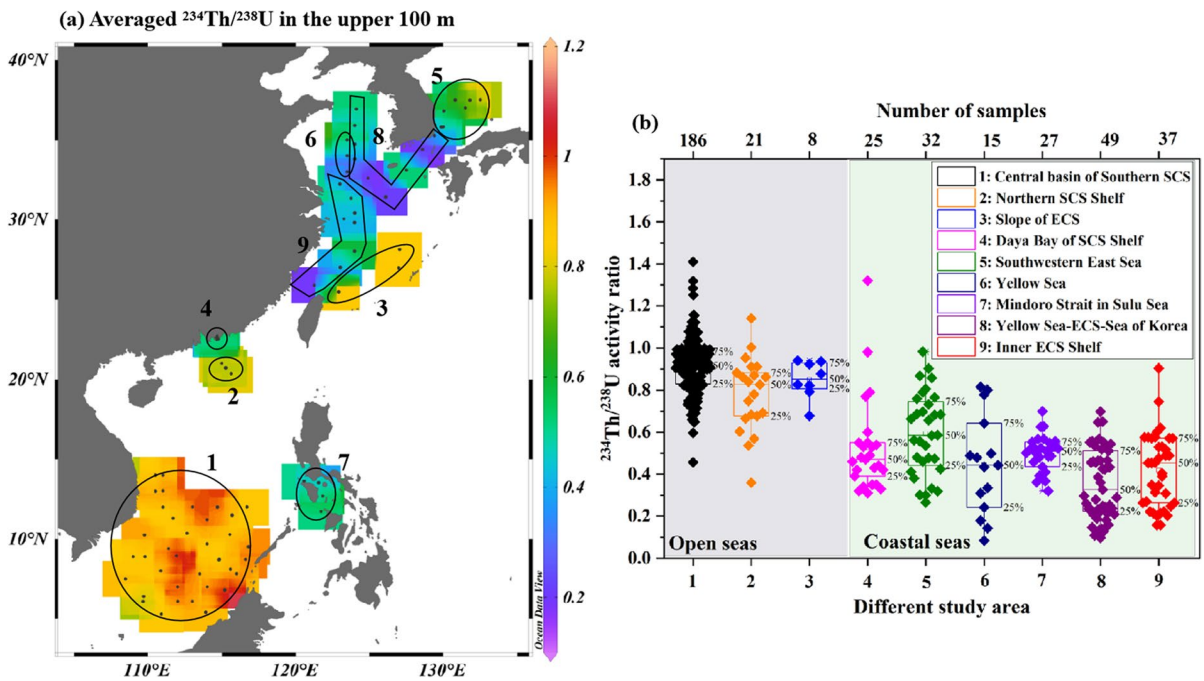

Fig. 6 **a** Spatial distribution of averaged $^{234}Th/^{238}U$ (activity ratios of ^{234}Th to ^{238}U) from the upper 100 m water column and (b) comparison of $^{234}Th/^{238}U$ (activity ratios of ^{234}Th to ^{238}U) in open seas and coastal seas near the ECS (East China Sea). Data was calculated from 1) the central basin of Southern South China Sea (SCS) (Cai et al. 2008); 2) the Northern SCS Shelf (Chen et al. 2008); 3) the continental slope of ECS (Bi et al. 2013); 4) the Daya Bay of northern SCS Shelf (Feng et al. 2021); 5) the southwestern East Sea (Kim et al. 2009); 6) the Yellow Sea (Zhao 2013); 7) the Mindoro Strait in Sulu Sea (Wei and Hung 1998), 8) the Yellow Sea-ECS-Sea of Korea (Seo et al. 2022), and 9) the Inner ECS Shelf (this study)

(0.426 ± 0.159, this study) were approximately two-fold higher than those in the Outer ECS shelf (0.850 ± 0.084, Bi et al. 2013). For the Southwestern East Sea, the averaged $^{234}Th/^{238}U$ ARs increased from 0.356 ± 0.082 at the nearshore station (station A2, ~ 100 m) to 0.918 ± 0.048 at the far shore basin station (station D4, ~ 2000 m) (Kim et al. 2009). In summary, unlike in open seas, the data revealed a distinct trend of enhanced depletion of ^{234}Th activity relative to ^{238}U in the water column of particle-rich shallow seas (Fig. 6b). This trend can be attributed to the potential resuspension of sediments and the dominance of both marine biogenic and terrestrial inorganic particles in higher quantities in water bodies with rich particles, such as continental shelf areas, compared to deep slopes or open sea areas. As a result, ^{234}Th undergoes a more intense scavenging-removal process in shallow shelf areas, leading to a stronger deficits of ^{234}Th relative to ^{238}U in shallow seawater.

Removal flux of ^{234}Th

The strong relationship between ^{234}Th deficit and particle sinking builds the foundation of applying ^{234}Th–^{238}U disequilibrium to evaluate particle dynamics in marine environments. The ^{234}Th deficit relative to ^{238}U reflects its removal from sea water column. Changes of ^{234}Th–T with time are given by (Savoye et al. 2006; Amiel and Cochran 2008; Feng et al. 2021):

$$\frac{\partial I_{Th}}{\partial t} = \lambda_{Th} I_U - \lambda_{Th} I_{Th} - F_{Th} + V \quad (1)$$

where I_{Th} and I_U are the inventories of the total ^{234}Th and ^{238}U from surface to the export interface in units of dpm/m^2, which are calculated through the trapezoid approximation method. λ_{Th} is the decay constant of ^{234}Th (0.0288 day^{-1}). F_{Th} is the net removal flux of total ^{234}Th by sinking particles in unit of dpm/m^2/day. V is the sum of physical processes (including upwelling, advective and diffusive influences, Savoye et al. 2006). Generally, in the coastal systems, there might exist upwelling process and which carries seawater from deeper layers with high ^{234}Th concentration to shallow waters where ^{234}Th deficiency was more severe. However, from Fig. 3, we can not observe the increase signal of ^{234}Th in the upper 0–30 m layers of the ECS, hence the potential upwelling process is ignored in this study. By assuming steady state ($\partial I_{Th}/\partial t = 0$) and neglecting advection and diffusion ($V = 0$) (Amiel and Cochran 2008; Cai et al. 2008; Luo et al. 2014), the net ^{234}Th removal flux at the base of the layer of interest is equal to the ^{234}Th deficit integrated over depth (I_U-I_{Th}) multiplied by the ^{234}Th decay constant. Thus, we obtained:

$$F_{Th} = \lambda_{Th} \int_0^z (A_U - A_{Th}) dz \quad (2)$$

where z is the depth of the export interface and A_{Th} and A_U are the the measured activity concentrations of the total ^{234}Th and ^{238}U (unit: dpm/L = 1000 dpm/m^3). From Fig. 4, there were strong ^{234}Th deficits in the whole water column of the entire Inner ECS Shelf, hence the deepest sampling layer can be selected as the export interface. To make more complete use of the ^{234}Th profiles, the integration of the ^{234}Th deficit was done to near bottom layer for shallow stations (< 50 m) and to 45–50 m layer for deep stations (> 50 m). Based on the above parameters, the residence time of ^{234Th}–T (τ_T, in the unit of d) can be calculated by F_{Th} and I_{Th} (i.e., $\tau_T = I_{Th}/F_{Th}$) and this residence time is an important parameter that describes the scavenging rate of total ^{234}Th from the water column by sinking particles.

Based on Eq. (2), the estimated residence times and removal fluxes of total ^{234}Th were displayed in Table 1 and Fig. 7. The export fluxes of ^{234}Th varied from 922 ± 34 to 2684 ± 400 dpm/m^2/day (Table 1), and almost all stations had F_{Th} flux values of > 1000 dpm/m^2/day (Cai et al. 2008), indicating relatively robust particle scavenging in the eutrophic Inner ECS Shelf. Significant differences in ^{234}Th removal fluxes were observed among the sites within the study area (Fig. 7). The northern shallow stations (A3-9, A6-11, and A8-4), which are close to the Changjiang Estuary and influenced by terrestrial particles from the Changjiang River, exhibited relatively constant ^{234}Th removal fluxes (comparable to 1500 dpm/m^2/day) (F_{Th} values of A3-9, A6-11, and A8-4 were 1562 ± 57, 1654 ± 57 and 1544 ± 51 dpm/m^2/day, respectively). In contrast, the southern area (from E1 to A8-7), including the three stations (E1, E2, and E3) located far from the Changjiang Estuary, showed higher ^{234}Th removal fluxes compared to the shallower stations in the north (from A8-7 to

Table 1 The calculated ^{234}Th deficits, residence times and export fluxes of ^{234}Th on the Inner ECS (East China Sea) Shelf

Station	Integrated depth	Inventory (dpm/m^2)		^{234}Th Deficit[c]	F_{Th}[d]	τ_{Th-T}[e]
	m	^{234}Th–T[a]	^{238}U[b]	dpm/m^2	dpm/m^2/day	d
E1	0–50	$(2.41\pm0.22)\times10^4$	$(1.18\pm0.02)\times10^5$	$(9.33\pm0.88)\times10^4$	$(2.68\pm0.40)\times10^3$	9.0 ± 1.6
E2	0–50	$(4.10\pm0.29)\times10^4$	$(1.18\pm0.02)\times10^5$	$(7.75\pm0.58)\times10^4$	$(2.23\pm0.22)\times10^3$	18.4 ± 2.2
E3	0–50	$(6.63\pm0.26)\times10^4$	$(1.19\pm0.02)\times10^5$	$(5.24\pm0.22)\times10^4$	$(1.51\pm0.09)\times10^3$	44.0 ± 3.2
A8-7	0–50	$(4.09\pm0.15)\times10^4$	$(1.08\pm0.02)\times10^5$	$(6.67\pm0.27)\times10^4$	$(1.92\pm0.07)\times10^3$	24.0 ± 1.1
A8-4	0–45	$(4.44\pm0.11)\times10^4$	$(9.81\pm0.14)\times10^4$	$(5.37\pm0.15)\times10^4$	$(1.54\pm0.05)\times10^3$	28.8 ± 1.2
A6-11	0–45	$(4.12\pm0.13)\times10^4$	$(9.87\pm0.15)\times10^4$	$(5.75\pm0.21)\times10^4$	$(1.65\pm0.06)\times10^3$	24.9 ± 1.2
A3-9	0–45	$(3.67\pm0.13)\times10^4$	$(9.10\pm0.14)\times10^4$	$(5.43\pm0.21)\times10^4$	$(1.56\pm0.06)\times10^3$	23.5 ± 1.2
A1-5	0–30	$(2.16\pm0.08)\times10^4$	$(5.36\pm0.09)\times10^4$	$(3.20\pm0.13)\times10^4$	$(9.22\pm0.34)\times10^2$	23.4 ± 1.2

[a]Denotes the calculated inventory of total ^{234}Th;

[b]Denotes the calculated inventory of ^{238}U;

[c]Denotes the calculated deficit inventory of ^{234}Th;

[d]Denotes the export fluxes of ^{234}Th;

[e]Denotes the calculated residence time of total ^{234}Th

A3-9) (Fig. 7), despite similar integration depths. The three stations (E1, E2, and E3) in the southern part of the Inner ECS Shelf and A8-7 are far from the Changjiang Estuary and less affected by large amount of terrestrial particulate matter. However, comparing with the three stations in the north (A3-9, A6-11 and A8-4), they maintained a larger ^{234}Th removal flux (Table 1 and Fig. 7), suggesting that in regions where the quantity of lithogenic particles is not dominant, the small amount of marine biogenic particles present in the water body may have a stronger ability to scavenge ^{234}Th and compensate for the deficit caused by the lack of particle quantity.

The calculated residence times of ^{234}Th–T showed great spatial differences (Table 1 and Fig. 7). The minimum of 9.0 ± 1.6 d occurred at station E1 and the maximum of 44.0 ± 3.2 d was observed at station E3. The τ_{Th-T} at the five stations in the north of the Inner ECS Shelf were relatively close, ranging from 23 to 29 days. These residence times in the Inner ECS Shelf were shorter than those reported for Daya Bay (38–72 days, Feng et al. 2021), but slightly longer than those observed in the Taiwan coastal sea area (mostly < 10 days, Wei et al. 2009). Based on a previous work in the Yellow Sea-East China Sea and southern Sea of Korea published by Seo et al. (2022), the residence times of total ^{234}Th were calculated to be 7.2–43.5 days (mean: 20.1 ± 12.6 days, n = 9). Seo et al, (2022)'s results are in good agreement with the τ_{Th-T} values in our study. However, the residence times of ^{234}Th–T was much longer in deep sea areas such as continental slope and sea basin. For example, according to the ^{234}Th–^{238}U disequilibrium reported by Ma et al. (2009) in the central basin of the South China Sea, the τ_{Th-T} values were calculated to be 29–228 days, with an average of 113 days. Similarly, Bi et al. (2013) reported that the averaged residence times of total ^{234}Th in the slope of the ECS were high up to 289 d. Overall, these findings suggest a general trend that the residence time of ^{234}Th in the upper seawater tends to increase with increasing offshore distance (namely, τ_{Th-T} values: nearshore water < shelf water < slope / basin water).

Calculation of fractions of marine and terrestrial carbon ($f_{mar,\ terr}$ values)

POC fluxes are classically estimated via ^{234}Th removal fluxes (F_{Th}) multiplied by the ratio of POC to ^{234}Th–P at the export interface as used by Buesseler et al. (1992, 2006), Hong et al. (2021), and Yang et al. (2022), i.e.:

$$F_{POC} = F_{Th} \times \left(\frac{POC}{^{234}Th - P} \right) \quad (3)$$

where F_{POC} is the export flux of POC (mmol C/m^2/day) and POC/^{234}Th–P is the ratio of POC to particulate ^{234}Th activity (μmol C/dpm) on sinking particles at the export interface (30 or 45 or 50 m for different

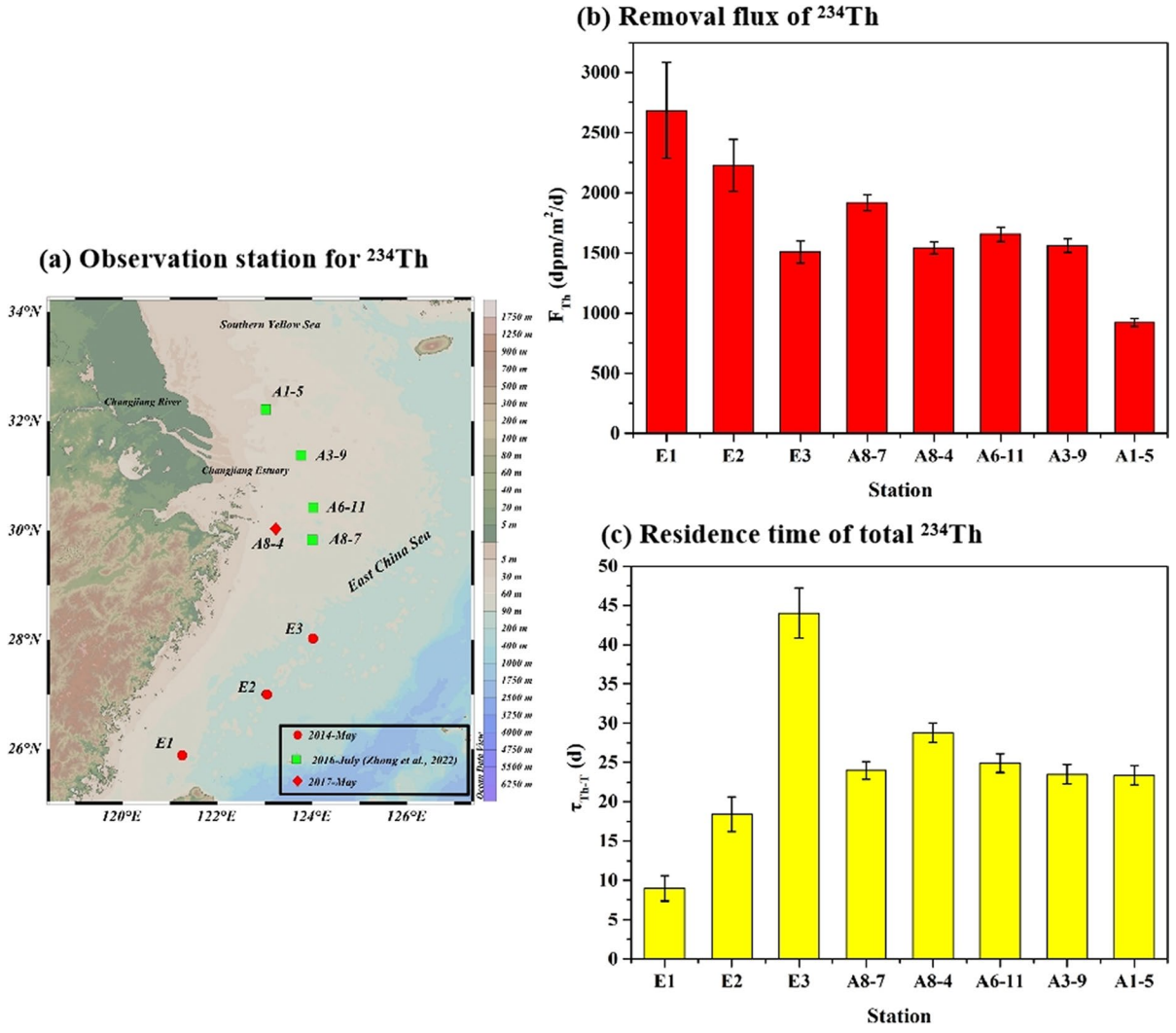

Fig. 7 Observation station (**a**), the calculated removal flux (F_{Th}) (**b**) and the residence time of ^{234}Th (τ_{Th-T}) (c) along the Transect A on the Inner ECS (East China Sea) Shelf (data cited from Table 1)

stations). Here, we use the same 0.45 µm QMA filters for total particle filtration and for POC measurement, hence, the > 0.45 µm-size fraction is taken as representative of the settling particles. Generally, the base of euphotic zone was used as the POC export interface. However, the euphotic zone or mixing layer was selected as the export interface of POC flux evaluation in our study because the water depth of the ECS shelf is relatively shallow (< 150 m) compared with that of the slope or basin area. According to the CTD measurement on the ship, the euphotic zone depths in this study area are in the range of 30–40 m (apart from station A1-5). And the mixing layer depths for the five northern stations (from A1-5 to A8-7) were 10–20 m and for the three southern stations (E1 to E3) were 20–30 m (Fig. 2). However, there were severe algal blooming in the northern stations, which caused the POC concentrations to rise to approximately 60 to > 100 µmol/L in the mixing layer (0–20 m) of these northern stations (Fig. 4a). Hence, if the mixing layers were selected as the export interface, the calculated POC fluxes would be several times higher than the POC flux obtained by selecting the base of euphotic zone as the export interface. Based on the above discussion, the base of euphotic zone (30–50 m

for different stations) was also selected as the export interface for POC flux evaluation.

The Inner ECS Shelf area has terrestrial as well as marine carbon sources. To distinguish and constrain the fluxes of marine and terrestrial POC, carbon stable isotope ($\delta^{13}C_{POC}$) can be used to resolve carbon source and the Eq. (3) can be modified accordingly (Amiel and Cochran 2008),

$$F_{POC}(mar\ or\ terr) = F_{Th} \times \left(\frac{POC}{^{234}Th - P}\right) \times f_{mar}\left(or\ f_{terr}\right) \quad (4)$$

where f_{mar} and f_{terr} are the fraction of marine and terrestrial carbon, respectively, in the > 0.45-μm fraction. It can be seen that in order to constrain the export fluxes of terrestrial POC or marine POC, the fraction of terrestrial (f_{terr}) or marine carbon (f_{mar}) in POC of all stations in the ECS shelf should be determined firstly. The relative abundance of f_{terr} can be estimated using a two-endmember isotopic mixing equation (Gõni et al. 2000; Amiel and Cochran 2008):

$$f_{terr} = \frac{\delta^{13}C_{POC} - \delta^{13}C_{mar}}{\delta^{13}C_{terr} - \delta^{13}C_{mar}} \quad (5)$$

where $\delta^{13}C_{terr}$ and $\delta^{13}C_{mar}$ are the isotopic signatures of terrestrial and marine POC endmembers; f_{terr} is the mass fraction of terrestrial carbon (thus, $f_{mar} = 1 - f_{terr}$), and $\delta^{13}C_{POC}$ is the measured $\delta^{13}C_{POC}$ values in samples obtained from the > 0.45-μm size fraction. For this calculation, the precision is controlled by the constraining of appropriate $\delta^{13}C$ values for marine and terrestrial endmembers.

The choice of representative $\delta^{13}C$ values for terrestrial ($\delta^{13}C_{terr}$) and marine ($\delta^{13}C_{mar}$) endmembers in studying the compositions of organic carbon in marine environments can be challenging due to various factors that can influence the carbon isotopic composition. Factors such as sewage modification, *in-situ* production, biological reworking of POC, hydrodynamic sorting, and different primary producer communities can lead to significant variations in the $\delta^{13}C$ values of terrestrial and marine endmembers (Jeffrey et al. 1983; Tan et al. 1991; Wu et al. 2003; Liu et al. 2007). Some previous studies have reported very changeable measured $\delta^{13}C_{POC}$ values for the terrestrial materials from the Changjiang River. Generally, the $\delta^{13}C$-POC in the freshwater endmember of Changjiang River was reported to vary from − 24‰ to -30.6‰ in different studies (Tan et al. 1991; Cai and Han 1999; Deng et al. 2006; Zhang et al. 2007). Considering these literature results, a mean $\delta^{13}C_{POC}$ value of − 27.7 ± 1.0‰, measured from the lower reaches of the Changjiang River, is often recommended as the representative $\delta^{13}C_{terr}$ endmember (Wu et al. 2003; Zhang et al. 2007; Seo et al. 2022). For the marine end-member $\delta^{13}C_{mar}$, a value of − 20.0 ± 1.0‰, as summarized by Zhang et al. (2007), is commonly used as a typical $\delta^{13}C_{mar}$ value in the ECS. This value is similar to the $\delta^{13}C_{mar}$ (-19.7‰) used by Seo et al. (2022) in their published work.

The calculated f_{terr} values ranged from (0 ± 2)% to (74 ± 5)%, and the range of f_{mar} determined from all samples is (25 ± 5)%-(100 ± 2)% (Fig. 8). The mean values of f_{terr} and f_{mar} in the whole water column were calculated to be 30 ± 22% and 70 ± 22%, respectively (Fig. 8), indicating that the majority of the POC in the > 0.45 μm fraction was of marine provenance (or in situ production) throughout the entire Inner ECS Shelf. Interestingly, higher f_{mar} values were found at the northern five stations (from A8-7 to A1-5) which are close to the Changjiang Estuary (Fig. 1). Despite receiving abundant terrestrial carbon input from the Changjiang River, this region exhibited higher f_{mar} values. As mentioned in Sect. 3.4, much higher POC concentration and $\delta^{13}C_{POC}$ values were also observed at these five stations in the north of the study area, indicating the presence of strong in situ production activities in this region. This finding is consistent with the occurrence of phytoplankton blooms in the late spring (May to June) in the northern region of the study area (Li et al. 2014; Yu et al. 2017).

POC export fluxes and carbon budget in the ECS Shelf

Using Eqs. (4) and (5), the marine and terrestrial POC fluxes were obtained in the Inner ECS Shelf (Table 2). It should be noted that in Table 2, the $\delta^{13}C$ value of the 30 m layer at station A1-5 was replaced by the result of the 15 m layer to elimimate the possible influence in the subsequent calculations, because the 30 m layer was strongly affected by sediment resuspension process (Zhong et al. 2022). The fluxes of marine POC at the southern three stations (E1, E2 and E3) ranged from 11 ± 2 to 54 ± 14 mmol C/m^2/day, with an average of 26 ± 20 mmol C/m^2/

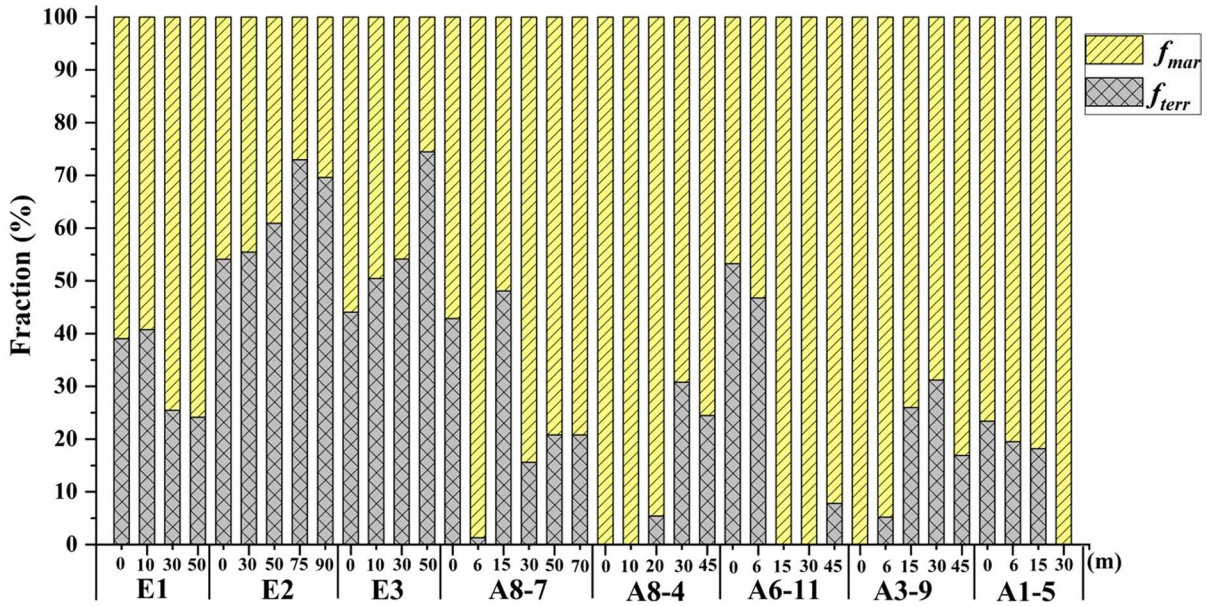

Fig. 8 Relative contribution of terrestrial and marine source to POC (particulate organic carbon). The f_{mar} and f_{terr} represent the percentage of marine and terrestrial organic carbon, respectively. The location of different station name can be found in Fig. 1

Table 2 The ratios of POC to particulate ^{234}Th (POC/^{234}Th–P) at the export interface and the estimated terrestrial (F_{POC}(terr)) and marine POC fluxes (F_{POC}(mar))

Station	Export interface	POC/^{234}Th–P	$\delta^{13}C_{POC}$ value	f_{terr}	f_{mar}	F_{POC}(terr)	F_{POC}(mar)
	m	μmol C/dpm	‰			mmol C/m^2/day	
E1	50	26.5 ± 6.5	− 21.9	24%	76%	17 ± 5	54 ± 14
E2	50	12.4 ± 2.0	− 24.7	61%	39%	17 ± 3	11 ± 2
E3	50	33.9 ± 8.7	− 25.7	74%	26%	38 ± 10	13 ± 3
A8-7	50	57.5 ± 3.4	− 21.6	21%	79%	23 ± 2	87 ± 6
A8-4	45	111 ± 10	− 21.9	24%	76%	42 ± 4	129 ± 12
A6-11	45	20.2 ± 1.2	− 20.6	8%	92%	2.6 ± 0.2	31 ± 2
A3-9	45	46.2 ± 2.7	− 21.3	17%	83%	12 ± 1	60 ± 4
A1-5	30	160 ± 9	− 21.4*	18%	82%	27 ± 2	121 ± 9

The $\delta^{13}C$ value at 30 m layer ($\delta^{13}C$ = -18.9 ‰) was replaced by the $\delta^{13}C$ value of POC at 15 m layer (− 21.4‰), because the POC at 30 m layer was strongly influenced by sediment re-suspension process (Zhong et al. 2022)

day. The fluxes of terrestrial POC varied from 17 ± 3 to 38 ± 10 mmol C/m^2/day, with a mean value of 24 ± 10 mmol C/m^2/day for the same region. In the northern part of the Inner ECS Shelf (from A8-7 to A1-5), higher fluxes of marine POC were observed (ranging from 31 ± 2 to 129 ± 12 mmol C/m^2/day, with an average of 86 ± 37 mmol C/m^2/day, Table 2). The average flux of terrestrial POC in the north was 21 ± 13 mmol C/m^2/day, which is slightly lower than that in the south (24 ± 10 mmol C/m^2/day) from the overall average level. However, from each sampling station, we can see that more stations in the northern region have higher terrestrial POC flux than that in the southern region. Differently, station E3 in the south has a abnormally higher terrestrial POC flux. And the corresponding f_{terr} values in the south are also obviously higher than those in the north, although the Changjiang River Estuary is in the

north. The possible reason is the southern stations (E1 to E3) were collected in May, 2014, with this being the time of the year when the dominating wind direction changes from north to south. The suspended particles in the southern region is largely the particles sourced from Changjiang River, which had been moved southwards in the previous winter season. A previous study also found that POC along the coast in May showed elevated terrestrial signal west of the front while more offshore marine signal prevails (Zhu et al. 2014).

The flux of marine POC is generally greater than the flux of terrestrial POC throughout the Inner ECS Shelf by factors of ~ 3 to 10 (except for stations E2 and E3). These results suggest that during the growth period of plankton (e.g., May–July), although the Inner ECS Shelf receives a significant amount of terrestrial material from the Changjiang River and other surrounding rivers, the marine POC flux accounts for a larger proportion of the total POC flux. The finding is consistent with previous studies, such as O'Brien et al. (2006), who reported greater marine than terrestrial POC fluxes in the Mackenzie Shelf of the Arctic Ocean during early summer. Various studies have reported averaged primary production of 33–63 mmol C/m^2/day in the ECS (Hama et al. 1997; Gong and Liu 2003; Yoo et al. 2019). However, Gong et al. (2003) pointed out that the primary production in the ECS exhibits significant spatial and seasonal variation, with summer primary production (78 ± 53 mmol C/m^2/day) being approximately three times higher than in other seasons. Seo et al. (2022) reported an averaged primary production of 106 ± 66 mmol C/m^2/day in the Yellow Sea-ECS-Sea of Korea in August 2020. Comparing these finding to the export fluxes of marine POC in the ECS Shelf (Table 2), it can be observed that they are slightly lower than or comparable to the level of primary productivity, particularly in the northern part of the study area (Gong et al. 2003; Seo et al. 2022).

In order to understand the carbon cycle in the Inner ECS Shelf area, the water column carbon export fluxes obtained in this study can be combined with data on carbon burial fluxes in the sediments. Previous studies revealed variable organic carbon burial fluxes in the ECS Shelf area, ranging from 1.1 to 2.5 mmol C/m^2/day (at the PN section in the ECS continental shelf) to 7.7–12.5 mmol C/m^2/day (in the Zhejiang-Fujian coastal mud area of the Inner ECS) (Oguri et al. 1997; Chen and Wang 1999; Sun et al. 2020). However, these studies are not systematic. The most comprehensive work on organic carbon burial in the ECS was done by Deng et al. (2006), and they found a decreasing trend from the northwestern part (e.g. 45.7 mmol C/m^2/day in the Changjiang Eastury Delta) to southeastern area (0.5 mmol C/m^2/day in the ECS Slope and Okinawa Trough), with a weighted average organic carbon burial flux of approximately 3.4 mmol C/m^2/day. In addition, Wang et al. (2020) also presented work on sedimentary OC burial flux in the estuarine-inner shelf areas of the ECS and reported an averaged bulk OC deposition flux of 5.7 mmol C/m^2/day, while the deposition fluxes of marine and terrestrial OC were 4.5 and 1.3 mmol C/m^2/day, respectively. Considering the spatial variability and inhomogeneity of organic carbon burial fluxes in the ECS, it can be inferred that the southern and northern regions of the Inner ECS Shelf would exhibit different organic carbon burial fluxes. Referring to the corresponding position of our sampling stations in Fig. 5b of Deng et al. (2006), we can estimate approximate burial fluxes of organic carbon. Specifically, the southern stations (E1, E2 and E3) are located in the area with an estimated organic carbon burial flux of 1.1–2.3 mmol C/m^2/day, while the other five stations (A8-7 to A1-5) in the northern Inner ECS Shelf are situated in the region with an estimated organic carbon burial flux of 6.8–11.4 mmol C/m^2/day. Therefore, the values of 1.1–2.3 mmol C/m^2/day and 6.8–11.4 mmol C/m^2/day can then be used as the representative organic carbon burial fluxes in the southern and northern region of our study, respectively.

Figure 9 presents a simple carbon balance of POC in the southern and northern regions of the Inner ECS Shelf. In the southern Inner ECS Shelf (Fig. 9a), the average marine POC flux is comparable to the average terrestrial POC flux, both being 24 ± 10 mmol C/m^2/day and 26 ± 20 mmol C/m^2/day, respectively. The overall average POC export flux from the upper water column is relatively high at 50 ± 18 mmol C/m^2/day. However, the POC burial fluxes in the underlying sediments is only about 2.2–4.6% of the overall average POC export fluxes (Fig. 9a). In the northern region of the Inner ECS Shelf, influenced by the nutrient rich Changjiang River Diluted Water (Fig. 9b), the average marine POC flux is 86 ± 37 mmol C/m^2/day, while the average terrestrial POC flux is 21 ± 13 mmol C/

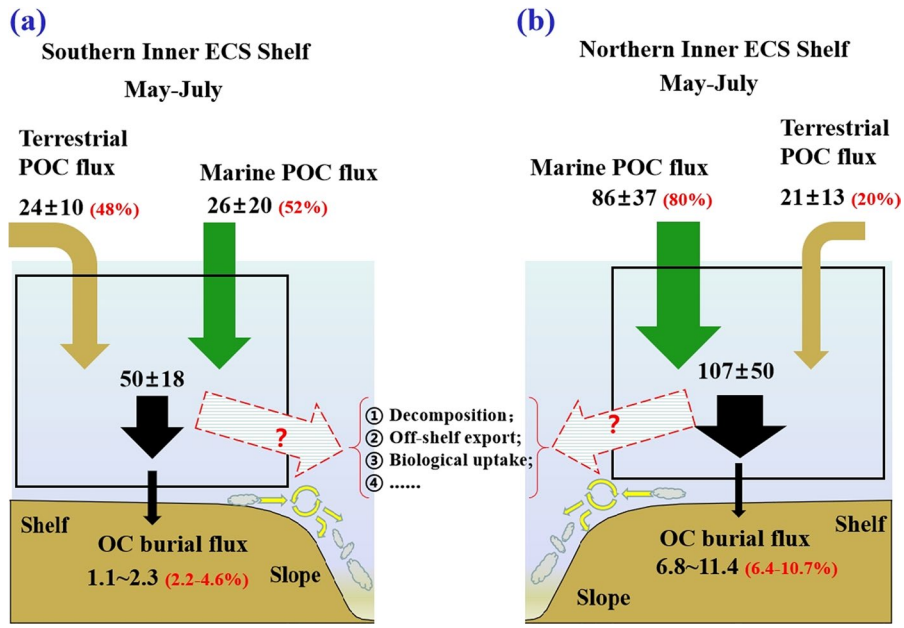

Fig. 9 A simple conceptual model of POC (particulate organic carbon) fluxes (mmol C/m^2/day) in the southern (**a**) and northern (**b**) Inner ECS Shelf. Organic carbon burial fluxes were obtained from Deng et al. (2006) according to the corresponding sampling location of our study. The % values in the figures represent the percentage of terrestrial or marine carbon fluxes in the total carbon export fluxes or the percentage of burial carbon in the total carbon export fluxes

m^2/day. Therefore, the average marine POC flux is approximately four times higher than the average terrestrial POC flux during the phytoplankton growth season. In this northern area, the sedimentary POC burial flux ranges from 6.8 to 11.4 mmol C/m^2/day, accounting for 6.4–10.7% of the total POC export fluxes from the entire water column (Fig. 9b). These results highlight the differences in carbon balance between the southern and northern regions of the Inner ECS Shelf. In the southern region, POC export from the water column dominates, with a relatively small contribution from sedimentary burial. In contrast, the northern region exhibits higher POC export fluxes, particularly in the marine fraction, and a larger proportion of POC is buried in the sediments.

In summary, the carbon cycle processes in the ECS Shelf exhibit distinct characteristics. One feature is that the POC burial efficiency in the northern region of the Inner ECS Shelf is higher (6.4–10.7%) compared to the southern region (2.2–4.6%). The five stations (including A8-7 to A1-5) in the northern region of the Inner ECS Shelf is characterized by high sediment accumulation rates (Deng et al. 2006; Qiao et al. 2017).This disparity can be attributed to the higher sediment accumulation rates observed in the northern area, which promotes the rapid burial and preservation of POC. The greater sediment flux in this region facilitates the entrapment and scavenging of POC, reducing its residence time in the water column. Additionally, the higher sedimentation rate ensures a greater amount of particles settling to the seafloor, leading to efficient storage of POC in the sediments and reducing the likelihood of POC being oxidized and degraded by zooplankton and bacteria. These findings suggest that increasing sedimentation rates can enhance the burial of bulk organic carbon (terrestrial + marine POC) in seabed sediments. Therefore, if it is feasible to induce phytoplankton blooms or trap terrestrial POC effectively in areas with high sedimentation rates, such as the Changjiang Estuary, it would be likely to serve as a viable approach to enhance ocean carbon sinks. By promoting the rapid sinking and burial of organic carbon, this method would probably contribute to long-term carbon storage in the sediments and mitigate its release into the atmosphere. However, it is important to consider potential ecological impacts and carefully manage such interventions to avoid detrimental effects on marine ecosystems.

Another important feature from Fig. 9 is the significant disparity between the export fluxes of marine, terrestrial, and overall POC and the burial fluxes of organic carbon in the sediments. Regardless of whether it is the southern or northern Inner ECS Shelf, the total POC export fluxes, as determined by ^{234}Th–^{238}U disequilibrium, are much higher

than the POC burial rates. In the northern Inner ECS Shelf, the total POC export fluxes are approximately 9 to 16 times higher than the POC burial rates (6.8–11.4 mmol C/m^2/day), while in the southern Inner ECS Shelf, the export fluxes are approximately 21 to 45 times higher than POC burial rates (1.1–2.3 mmol C/m^2/day). These findings suggest that a large proportion (> 90%) of terrestrial organic carbon and organic carbon from primary production, which is exported from the upper water column to the seafloor in the ECS Shelf, does not appear to be incorporated or preserved in the bottom sediments. In other words, most of the settled POC seems to be "lost". A recent study based on sediment oxygen consumption (SOC) measurement found approximately 87% of the organic carbon was decomposed in the water column and the sediment in the ECS (Song et al. 2016), which is consistent with our assessment result. This discrepancy between POC export and burial implies that there are additional processes or pathways through which the exported POC is either remineralized or transported to other regions before it can be incorporated into sediments. Decomposition refers to the microbial breakdown of organic matter into inorganic forms, such as carbon dioxide, which can then re-enter the water column and potentially be released back into the atmosphere. Alternatively, the exported POC may be transported to other areas beyond the study region, where it can be buried or undergo different fate processes. Furthermore, biological uptake and trophic transfer by zooplankton and benthic biomass can also be a possible process that cannot be ignored. The following section presents a specific discussion of the above three processes.

Sinking particles can be decomposed by microbes, plankton, or nekton. In shelf water, sediment resuspension and resettlement can facilitate aerobic decomposition of POC, which result in the great release of dissolved organic carbon (DOC) and inorganic nutrients (DIN, DIP, and DSi) into the water column (Chen and Wang 1999; Ogawa et al. 2003; Kim et al. 2020; Seo et al. 2022). Previous studies evaluated that 75–90% of organic carbon were degraded by biological processes in the ECS Shelf (Chen and Wang 1999; Deng et al. 2006; Seo et al. 2022). Secondly, "off-shelf export" of newly deposited POC (in the form of marine nepheloid layers and near-bottom outflows) from the ECS Shelf to the Okinawa Trough through the slope can also be an important mechanism for "carbon missing" (Chen and Wang 1999; Oguri et al. 2003; Deng et al. 2006). It has been estimated that this cross-boundary transportation accounts for approximately 5% of the organic carbon transported to the continental slope (Chen 2010; Song et al. 2016). Lastly, for biological uptake of POC, sinking and newly deposited particles can be consumed by zooplankton, swimmers, or benthic organisms and then these marine organism might migrate away from the ECS Shelf to other areas of the ocean. However, quantifying the transfer of POC into marine biomass posses challenges, and no work quantitatively assess the contributions of the biological carbon transfer in the ECS Shelf. Hence, in summary, the most important process causing the carbon missing in the ECS Shelf is presumed to be biodegradation.

Summary and conclusion

In the large river-dominated ECS Shelf water, the ^{234}Th–^{238}U disequilibrium and stable carbon isotopic composition (δ^{13}C) of POC were measured to differentiate between terrestrial and marine POC export fluxes. The concentrations of POC ranged from 2.54 to 199 μmol/L, with significantly higher concentrations in the northern Inner ECS Shelf due to the presence of abundant phytoplankton biomass influenced by the nutrient rich Changjiang River. Using a two-end-member mixing model based on the δ^{13}C values, it was determined that the majority of POC in the entire shelf water primarily originated from marine sources (or *in-situ* production), especially in the northern part of the study area. The ^{234}Th–^{238}U disequilibrium analysis revealed significant deficiencies of ^{234}Th relative to ^{238}U throughout the water column at all stations. This was indicated by ^{234}Th/^{238}U activity ratio consistently being less than unity (from 0.158 ± 0.045 to 0.904 ± 0.068, averaging 0.426 ± 0.159).

Fluxes of marine POC and terrestrial POC settling to the seafloor in the ECS Shelf exhibited a wide range, varying from 11 to 129 mmol C/m^2/day and from 2.6 to 38 mmol C/m^2/day, respectively, showing a significant spatial variability among different stations. The averaged fluxes of terrestrial POC in the southern and northern ECS Shelf were relatively similar, ranging from ~ 21 to 24 mmol C/

m^2/day. However, the averaged flux of marine POC in the northern region (86 ± 37 mmol C/m^2/day) was much higher compared to that of the southern region (26 ± 20 mmol C/m^2/day), which can be attributed to the higher primary production frequently observed in the northern Inner ECS Shelf. The northern Inner ECS Shelf, characterized by higher sedimentation rates and higher fluxes of marine POC, exhibited a higher carbon burial efficiency. By constructing simple carbon budgets in the northern and southern ECS Shelf, it was found that over 90% of POC exported from the upper seawater would be missing until stable burial and the main process causing carbon missing is presumed to be the highly efficient microbial decomposition.

Acknowledgements This work was supported by the National Key R&D Program of China (2022YFE0209300) and the National Natural Science Foundation of China (No. 42206166, 42307280 and 42107251). The first author is very grateful to Ms. Yuehua Zhou for her care during his three-year post-doctoral work period.

Author Contributions Qiangqiang Zhong conceived and designed the study; Dekun Huang and Qiangqiang Zhong performed chemical analyses and provided data; Qiangqiang Zhong, Qiugui Wang, Jinzhou Du, Fule Zhang and Jinglin wrote the manuscript; Tao Yu provided polishing language and open access fees.

Funding This study was funded by the National Key R&D Program of China (2022YFE0209300), Jinzhou Du and the National Natural Science Foundation of China (No. 42206166, Qiangqiang Zhong and 42307280, Qiugui Wang).

Data availability All data generated during the current study are included in this published article and are available from the corresponding author on reasonable request.

Declarations

Conflict of Interests The authors declare that we do not have any commercial or associative interest that represents a conflict of interest in connection with the work submitted.

References

Amiel D, Cochran JK (2008) Terrestrial and marine POC fluxes derived from ^{234}Th distributions and δ^{13}C measurements on the Mackenzie Shelf. J Geophys Res 113:C03S06. https://doi.org/10.1029/2007JC004260

Bi Q, Du J, Wu Y, Zhou J, Zhang J (2013) Particulate organic carbon export flux by ^{234}Th/^{238}U disequilibrium in the continental slope of the East China Sea. Acta Oceanol Sin 32(10):67–73. https://doi.org/10.1007/s13131-013-0303-7

Black EE, Lam PJ, Lee J-M, Buesseler KO (2019) Insights from the ^{238}U–^{234}Th method into the coupling of biological export and the cycling of cadmium, cobalt, and manganese in the Southeast Pacific Ocean. Glob Biogeochem Cycles 33:15–36. https://doi.org/10.1029/2018gb005985

Buesseler KO, Boyd PW (2009) Shedding light on processes that control particle export and flux attenuation in the twilight zone of the open ocean. Limnol Oceanogr 54(4):1210–1232

Buesseler KO, Bacon MP, Cochran JK, Livingston HD (1992) Carbon and nitrogen export during the JGOFS North Atlantic Bloom experiment estimated from ^{234}Th:^{238}U disequilibria. Deep Sea Res Part I 39(7–8):1115–1137

Buesseler KO, Benitez-Nelson CR, Rutgers van der Loeff M, Andrew J, Ball L, Crossin G, Charette MA (2001) An intercomparison of small- and large-volume techniques for thorium-234 in seawater. Mar Chem 74(1):15–28

Buesseler KO, Benitez-Nelson CR, Moran SB, Burd A, Charette M, Cochran JK, Coppola L, Fisher NS, Fowler SW, Gardner WD, Guo LD, Gustafsson O, Lamborg C, Masque P, Miquel JC, Passow U, Santschi PH, Savoye N, Stewart G, Trull T (2006) An assessment of particulate organic carbon to thorium-234 ratios in the ocean and their impact on the application of ^{234}Th as a POC flux proxy. Mar Chem 100(3–4):213–233

Buesseler KO, Antia AN, Chen M, Fowler SW, Gardner WD, Gustafsson O, Harada K, Michaels AF, Rutgers van der Loeff M, Sarin M, Steinberg DK, Trull T (2007) An assessment of the use of sediment traps for estimating upper ocean particle fluxes. J Mar Res 65(3):345–416

Buesseler KO, Benitez-Nelson CR, Roca-Martí M, Wyatt AM, Resplandy L, Clevenger SJ, Drysdale JA, Estapa ML, Pike S, Umhau BP (2020) High-resolution spatial and temporal measurements of particulate organic carbon flux using ^{234}Th in the northeast Pacific Ocean during the export processes in the ocean from RemoTe Sensing field campaign. Elem Sci Anth 8(1):030. https://doi.org/10.1525/elementa.030

Burdige DJ (2005) Burial of terrestrial organic matter in marine sediments: a reassessment. Global Biogeochem Cycles 19(4):1–7

Cai DL, Han YB (1998) Carbon isotopic composition and flux of particulate organic matter in the Changjiang. Acta Oceanol Sin 17:337–342

Cai P, Dai M, Lv D, Chen W (2006) An improvement in the small-volume technique for determining thorium-234 in

seawater. Mar Chem 100(3–4):282–288. https://doi.org/10.1016/j.marchem.2005.10.016
Cai P, Chen W, Dai M, Wan Z, Wang D, Li Q, Tang T, Lv D (2008) A high-resolution study of particle export in the southern South China Sea based on ^{234}Th:^{238}U disequilibrium. J Geophys Res Oceans 113(C4):535–547
Chen CTA, Wang SL (1999) Carbon, alkalinity and nutrient budgets on the East China Sea continental shelf. J Geophys Res Oceans 104:20675–20686
Chen W, Cai P, Dai M, Wei J (2008) ^{234}Th/^{238}U disequilibrium and particulate organic carbon export in the Northern South China Sea. J Oceanogr 64(3):417–428
Chen C-TA (2010) Cross-boundary exchanges of carbon and nitrogen in continental margins. In: Liu KK et al (eds) Carbon and nutrient fluxes in continental margins. Springer-Verlag, Berlin, pp 561–574
Cheng H (2020) Future earth and sustainable developments. Innovation 1(100055):1–2. https://doi.org/10.1016/j.xinn.2020.100055
Deng B, Zhang J, Wu Y (2006) Recent sediment accumulation and carbon burial in the East China Sea. Glob Biogeochem Cycl 20:3014. https://doi.org/10.1029/2005GB002559
Djogić R, Sipos L, Branica M (1986) Characterization of uranium (VI) in seawater. Limnol Oceanogr 31(5):1122–1131
Eppley RW, Peterson BJ (1979) Particulate organic matter flux and planktonic new production in the deep ocean. Nature 282:677–680
Feng N, Yang W, Zhao X, Chen M, Qiu Y, Zheng M (2021) Seasonal export of ^{234}Th and POC in Daya Bay, northern South China Sea. Cont Shelf Res 216:104359
Friedlingstein P, O'Sullivan M, Jones MW, Andrew RM, Hauck J, Olsen A, Peters GP, Peters W, Pongratz J, Sitch S, Le Quéré C, Canadell JG, Ciais P, Jackson RB, Alin S, Aragão LEOC, Arneth A, Arora V, Bates NR, Becker M, Benoit-Cattin A, Bittig HC, Bopp L, Bultan S, Chandra N, Chevallier F, Chini LP, Evans W, Florentie L, Forster PM, Gasser T, Gehlen M, Gilfillan D, Gkritzalis T, Gregor L, Gruber N, Harris I, Hartung K, Haverd V, Houghton RA, Ilyina T, Jain AK, Joetzjer E, Kadono K, Kato E, Kitidis V, Korsbakken JI, Landschützer P, Lefèvre N, Lenton A, Lienert S, Liu Z, Lombardozzi D, Marland G, Metzl N, Munro DR, Nabel JEMS, Nakaoka S-I, Niwa Y, O'Brien K, Ono T, Palmer PI, Pierrot D, Poulter B, Resplandy L, Robertson E, Rödenbeck C, Schwinger J, Séférian R, Skjelvan I, Smith AJP, Sutton AJ, Tanhua T, Tans PP, Tian H, Tilbrook B, van der Werf G, Vuichard N, Walker AP, Wanninkhof R, Watson AJ, Willis D, Wiltshire AJ, Yuan W, Yue X, Zaehle S (2020) Global Carbon Budget 2020. Earth Syst Sci Data 12:3269–3340. https://doi.org/10.5194/essd-12-3269-2020
Gong GC, Liu GJ (2003) An empirical primary production model for the East China Sea. Cont Shelf Res 23:213–224
Gong GC, Wen YH, Wang BW, Liu GJ (2003) Seasonal variation of chlorophyll a concentration, primary production and environmental conditions in the subtropical East China Sea. Deep Sea Res Part II 50(6/7):1219–1236
Gõni MA, Yunker MB, Macdonald R, Eglington T (2000) Distribution of organic biomarkers in Arctic sediments from the Mackenzie River and Beaufort Shelf. Mar Chem 71:23–51
Hama T, Shin KH, Handa N (1997) Spatial variability in the primary productivity in the East China Sea and its adjacent waters. J Oceanogr 53:41–51
Hedges JI, Keil RG (1995) Sedimentary organic matter preservation: an assessment and speculative synthesis. Mar Chem 49(2–3):81–115
Hedges JI, Clark WA, Come GL (1988) Organic matter sources to the water column and surficial sediments of a marine bay. Limnol Oceanogr 33(5):1116–1136
Hong Q, Peng S, Zhao D, Cai P (2021) Cross-shelf export of particulate organic carbon in the northern South China Sea: insights from a ^{234}Th mass balance. Prog Oceanogr 193:102532. https://doi.org/10.1016/j.pocean.2021.102532
Jeffrey AWA, Brooks JM, Pflaum RC, Sackett WM (1983) Vertical trends in particulate organic-carbon ^{13}C:^{12}C ratios in the upper water column. Deep-Sea Res 30:971–983
Kim D, Choi M-S, Oh H-Y, Kim KH, Hon J-H (2009) Estimate of particulate organic carbon export flux using ^{234}Th/^{238}U disequilibrium in the Southwestern East Sea during summer (In Korean with English Abstract). The Sea 14(1):1–9
Kim J, Kim TH, Park SR, Lee HJ, Kim JK (2020) Factors controlling the distributions of dissolved organic matter in the East China Sea during summer. Sci Rep 10(1):11854. https://doi.org/10.1038/s41598-020-68863-w
Li HM, Tang HJ, Shi XY, Zhang CS, Wang XL (2014) Increased nutrient loads from the Changjiang (Yangtze) River have led to increased Harmful Algal Blooms. Harmful Algae 39:92–101
Liu K-K, Kao S-J, Hu H-C, Chou W-C, Hung G-W, Tseng C-M (2007) Carbon isotopic composition of suspended and sinking particulate organic matter in the northern South China Sea—From production to deposition. Deep Sea Res II 54:1504–1527
Liu Z, Deng Z, He G, Wang H, Zhang X, Lin J, Qi Y, Liang X (2022) Challenges and opportunities for carbon neutrality in China. Nat Rev Earth Environ 3:141–155
Liu S, Li D-W, Xiang R, Yu M, Zhang H, Li L, Zhao M (2023) Intensification of the East Asian winter monsoon resulted in greater preservation of terrestrial organic carbon on the inner shelf of the East China Sea since the last 1400 years. Palaeogeogr Palaeoclimatol Palaeoecol 615:111454
Luo Y, Miller LA, De Baere B, Soon M, Francois R (2014) POC fluxes measured by sediment traps and ^{234}Th:^{238}U disequilibrium in Saanich Inlet, British Columbia. Mar Chem 162:19–29
Milliman JD, Meade RH (1983) World-wide delivery of river sediment to the oceans. J Geol 91(1):1–21. https://doi.org/10.1086/628741
Muller-Karger FE, Varela R, Thunell R, Luerssen R, Hu C, Walsh JJ (2005) The importance of continental margins in the global carbon cycle. Geophys Res Lett 32:L01602. https://doi.org/10.1029/2004GL021346
Ning X, Liu Z, Shi J (1995) Primary production and the potential fish production in Bohai Sea, Yellow Sea and the East China seas. Acta Oceanol Sin (In Chinese with English Abstract) 17:72–84
O'Brien MC, Macdonald RW, Melling H, Iseki K (2006) Particle fluxes and geochemistry on the Canadian Beaufort Shelf: implications for sediment transport and deposition. Cont Shelf Res 26:41–81

Ogawa H, Usui T, Koike I (2003) Distribution of dissolved organic carbon in the East China Sea. Deep Sea Res Part II 50:353–366

Oguri K, Matsumoto E, Yamada M, Saito Y, Iseki K (2003) Sediment accumulation rates and budgets of depositing particles of the East China Sea. Deep Sea Res Part II 50:513–528

Oguri K, Matsumoto E, Saito Y, Hama T, Yamada M, Narita H, Iseki K (1997) Rates of sediment accumulation and carbon burial measured with ^{210}Pb in the East China Sea. Proceedings of the International Marine Science Symposium on Biogeochemical Processes in the North Pacific, edited by Tsunogai, S., pp 360–367, Japan Marine Science Foundation, Tokyo

Owens SA, Buesseler KO, Sims KWW (2011) Re-evaluating the ^{238}U-salinity relationship in seawater: Implications for the ^{238}U–^{234}Th disequilibrium method. Mar Chem 127(1–4):31–39. https://doi.org/10.1016/j.marchem.2011.07.005

Pike SM, Buesseler KO, Andrews J, Savoye N (2005) Quantification of ^{234}Th recovery in small volume sea water samples by inductively coupled plasma-mass spectrometry. J Radioanal Nucl Chem 263(2):355–360. https://doi.org/10.1007/s10967-005-0594-z

Qiao SQ, Shi XF, Wang GQ, Zhou X, Hu BQ, Hu LM, Yang G, Liu YG, Yao ZQ, Liu SF (2017) Sediment accumulation and budget in the Bohai Sea, Yellow Sea and East China Sea. Mar Geol 390:270–281

Santschi PH, Murray JW, Baskaran M, Benitez-Nelson CR, Guo LD, Hung C-C, Lamborg C, Moran SB, Passow U, Roy-Barman M (2006) Thorium speciation in seawater. Mar Chem 100(3–4):250–268

Savoye N, Benitez-Nelson C, Burd AB, Cochran JK, Charette M, Buesseler KO, Jackson GA, Roy-Barman M, Schmidt S, Elskens M (2006) ^{234}Th sorption and export models in the water column: a review. Mar Chem 100(3–4):234–249

Schlitzer R (2020) Ocean Data View, odv.awi.de.

Seo J, Kim G, Hwang J (2022) Sources and behavior of particulate organic carbon in the Yellow Sea and the East China Sea Based on ^{13}C, ^{14}C, and ^{234}Th. Front Mar Sci 9:793556. https://doi.org/10.3389/fmars.2022.793556

Shen Z-L, Liu Q (2009) Nutrients in the Changjiang River. Environ Monit Assess 153:27–44

Song G, Liu S, Zhu Z, Zhai W, Zhu C, Zhang J (2016) Sediment oxygen consumption and benthic organic carbon mineralization on the continental shelves of the East China Sea and the Yellow Sea. Deep-Sea Res Part II 124:53–63

Song J, Qu B, Li X, Yuan H, Li N, Duan L (2018) Carbon sinks/sources in the Yellow and East China Seas-Air-sea interface exchange, dissolution in seawater, and burial in sediments. Sci China Earth Sci 61(11):1583–1593

Su J (2001) A review of circulation dynamics of the coastal oceans near China. Haiyang Xuebao (in Chinese with English Abstract) 23(4):1–16

Sun X, Fan D, Liu M, Liao H, Tian Y (2020) The fate of organic carbon burial in the river-dominated East China Sea: Evidence from sediment geochemical records of the last 70 years. Org Geochem 143:103999. https://doi.org/10.1016/j.orggeochem.2020.103999

Tan FC, Cai DL, Edmond JM (1991) Carbon isotope geochemistry of the Changjiang Estuary. Estuar Coast Shelf Sci 32:395–403

Wang XC, Sun MY, Li AC (2008) Contrasting chemical and isotopic compositions of organic matter in Changjiang (Yangtze river) Estuarine and East China Sea shelf sediments. J Oceanogr 64(2):311–321

Wang X, Ma H, Li R, Song Z, Wu J (2012) Seasonal fluxes and source variation of organic carbon transported by two major Chinese Rivers: the Yellow River and Changjiang (Yangtze) River. Glob Biogeochem Cycles 26:GB2025

Wang C, Hao Z, Gao J, Feng Z, Ding Y, Zhang C, Zou X (2020) Reservoir construction has reduced organic carbon deposition in the East China Sea by half since 2006. Geophys Res Lett. https://doi.org/10.1029/2020GL087357

Wei C-L, Hung C-C (1998) Particle scavenging in the upper water column off Mindoro Island, Philippine: ^{234}Th/^{238}U Disequilibria. Estuar Coast Shelf Sci 46:351–358

Wei C-L, Tsai J-R, Wen L-S, Pai S-C, Tai J-H (2009) Nearshore scavenging phenomenon elucidated by ^{234}Th/^{238}U disequilibrium in the coastal waters off Western Taiwan. J Oceanogr 65:137–150. https://doi.org/10.1007/s10872-009-0014-z

Wu Y, Zhang J, Li DJ, Wei H, Lu RX (2003) Isotope variability of particulate organic matter at the PN section in the East China Sea. Biogeochemistry 65(1):31–49

Xu F, Hu B, Yuan S, Zhao Y, Dou Y, Jiang Z, Yin X (2018) Heavy metals in surface sediments of the continental shelf of the South Yellow Sea and East China Sea: sources, distribution and contamination. CATENA 160:194–200

Yang W, Zhao X, Chen M, Qiu Y, Zheng M (2022) Lagrangian observation of ^{234}Th and its application in constraining the sinking of particulate organic carbon on the slope of the Northeastern South China Sea. Front Mar Sci 9:831937. https://doi.org/10.3389/fmars.2022.831937

Yao P, Yu Z, Bianchi TS, Guo Z, Zhao M, Knappy CS, Keely BJ, Zhao B, Zhang T, Pan H, Wang J, Li D (2015) A multiproxy analysis of sedimentary organic carbon in the Changjiang Estuary and adjacent shelf. J Geophys Res Biogeosci 120:1407–1429. https://doi.org/10.1002/2014JG002831

Yoo S, Kong CE, Son YB, Ishizaka J (2019) A critical reassessment of the primary productivity of the Yellow Sea, East China Sea and Sea of Japan/East Sea Large Marine Ecosystems. Deep-Sea Res Part II 163:6–15

Yu RC, Zhang QC, Kong FZ, Zhou ZX, Chen ZF, Zhao Y, Geng HX, Dai L, Yan T, Zhou MJ (2017) Status, impacts and long-term changes of harmful algal blooms in the sea area adjacent to the Changjiang River Estuary (In Chinese with English Abstract). Oceanol Limnol Sin 48(6):1178–1186

Zhang J, Wu Y, Jennerjahn TC, Ittekkot V, He Q (2007) Distribution of organic matter in the Changjiang (Yangtze River) Estuary and their stable carbon and nitrogen isotopic ratios: Implications for source discrimination and sedimentary dynamics. Mar Chem 106:111–126

Zhao D (2013) A study of particulate organic carbon export in the yellow sea in summer based on ^{234}Th:^{238}U disequilibrium (In Chinese with English Abstract). Clim Chang Res Lett 2:159–164

Zhong Q, Li L, Puigcorbé V, Huang D, Yu T, Du J (2022) Contrasting behaviors of ^{210}Po, ^{210}Pb and ^{234}Th in the East China Sea during a severe red tide: Enhanced scavenging and promoted fractionation. Acta Oceanol Sin 41(8):5–21

Zhou F, Xue H, Huang D, Xuan J, Ni X, Xiu P, Hao Q (2015) Crossshelf exchange in the shelf of the East China Sea. J Geophys Res Oceans 120(3):1545–1572. https://doi.org/10.1002/2014JC010567

Zhu ZY, Zhang J, Wu Y, Lin J (2006) Bulk particulate organic carbon in the East China Sea: tidal influence and bottom transport. Prog Oceanogr 69:37–60

Zhu ZY, Wu Y, Zhang J, Dittmar T, Li Y, Shao L, Ji Q (2014) Can primary production contribute non-labile organic matter in the sea: amino acid enantiomers along the coast south of the Changjiang Estuary in May. J Marine Syst 129:343–349